Chemico-Biological Interactions 254 (2016) 34–44

Contents lists available at ScienceDirect

Chemico-Biological Interactions

journal homepage: www.elsevier.com/locate/chembioint

Indirect effects of TiO_2 nanoparticle on neuron-glial cell interactions

I-Lun Hsiao, Chia-Cheng Chang, Chung-Yi Wu, Yi-Kong Hsieh, Chun-Yu Chuang, Chu-Fang Wang, Yuh-Jeen Huang*

Department of Biomedical Engineering and Environmental Sciences, National Tsing Hua University, No. 101, Section 2, Kuang-Fu Road, Hsinchu 30013, Taiwan

ARTICLE INFO

Article history:
Received 1 March 2016
Received in revised form
24 April 2016
Accepted 19 May 2016
Available online 20 May 2016

Keywords:
Titanium dioxide nanoparticles
Co-culture
Uptake mechanisms
Reactive oxygen species
Cytokines
Central nervous system

ABSTRACT

Although, titanium dioxide nanoparticles (TiO_2NPs) are nanomaterials commonly used in consumer products, little is known about their hazardous effects, especially on central nervous systems. To examine this issue, ALT astrocyte-like, BV-2 microglia and differentiated N2a neuroblastoma cells were exposed to 6 nm of 100% anatase TiO_2NPs. A lipopolysaccharide (LPS) was pre-treated to activate glial cells before NP treatment for mimicking NP exposure under brain injury. We found that ALT and BV-2 cells took up more NPs than N2a cells and caused lower cell viability. TiO_2NPs induced IL-1β in the three cell lines and IL-6 in N2a. LPS-activated BV-2 took up more TiO_2NPs than normal BV-2 and released more intra/extracellular reactive oxygen species (ROS), IL-1β, IL-6 and MCP-1 than did activated BV-2. Involvement of clathrin- and caveolae-dependent endocytosis in ALT and clathrin-dependent endocytosis and phagocytosis in BV-2 both had a slow NP translocation rate to lysosome, which may cause slow ROS production (after 24 h). Although TiO_2NPs did not directly cause N2a viability loss, by indirect NP exposure to the bottom chamber of LPS-activated BV-2 in the Transwell system, they caused late apoptosis and loss of cell viability in the upper N2a chamber due to H_2O_2 and/or TNF-α release from BV-2. However, none of the adverse effects in N2a or BV-2 cells was observed when TiO_2NPs were exposed to ALT-N2a or ALT-BV-2 co-culture. These results demonstrate that neuron damage can result from TiO_2NP-mediated ROS and/or cytokines release from microglia, but not from astrocytes.

1. Introduction

Titanium dioxide nanoparticles (TiO_2NPs), due to good antimicrobial activity and high UV-absorption, are frequently used in personal-care products, such as sunscreens, lotions, shampoos, lip balm and toothpaste, or even as a food additive [1–6]. As a result of their prevalence, many studies have evaluated potential toxicity and toxic mechanisms of TiO_2NPs through *in vivo* and *in vitro* studies in order to understand safety risks to humans [7].

In vivo studies have indicated that TiO_2NPs would translocate into central nervous system (CNS) and have been detected in brain, mainly in the hippocampus, introduced by oral [8], intragastric [9] or intravenous (IV) injection [10,11]. Compared with other organs (liver, spleen, lung and kidney), the level of NP translocation to brain was relatively low [10]. However, NPs might exhibit a longer half-life in brain than in other organs. For instance, 80–150 nm TiO_2NPs could be detected in brain after 5 days of repeated intravenously applied doses and for 90 days of recovery [10]. Exposure to 5 nm of anatase TiO_2NPs in mouse brain resulted in decreased enzyme activity and neurotransmitter release, increased inflammation in gene expression (TNF-α, NF-κB, IL-1β, etc.), and significantly impaired spatial memory behavior [9,12]. Therefore, potential health risks to the brain exist when exposed to TiO_2NPs.

The brain consists of neurons and other glial cells (astrocytes, microglia, and oligodendrocytes). To recognize mechanisms of nanoparticle-induced neurotoxicity, the individual effect of TiO_2NPs on each kind of cell has been studied [13–17]. For example, 25 nm of anatase TiO_2NPs induced S-phase cell-cycle arrest,

Abbreviations: TiO_2NPs, titanium dioxide nanoparticles; LPS, Lipopolysaccharides; ROS, reactive oxygen species; CNS, central nervous system; AD, Alzheimer's disease; PD, Parkinson's disease; Aβ, amyloid-β; iNOS, inducible nitric oxide synthase; TEM, transmission electron microscope; IBMX, isobutylmethylxanthine; FI, fluorescence intensity; CPZ, chlorpromazine hydrochloride; MDC, monodansylcadaverine; PAO, phenylarsine oxide; ICP-MS, inductively coupled plasma mass spectrometry.

* Corresponding author.
E-mail addresses: ilunshiou@gmail.com (I.-L. Hsiao), a03039595@hotmail.com (C.-C. Chang), s9812805@m98.nthu.edu.tw (C.-Y. Wu), d944530@oz.nthu.edu.tw (Y.-K. Hsieh), cychuang@mx.nthu.edu.tw (C.-Y. Chuang), cfwang@mx.nthu.edu.tw (C.-F. Wang), yjhuang@mx.nthu.edu.tw (Y.-J. Huang).

http://dx.doi.org/10.1016/j.cbi.2016.05.024
0009-2797/

apoptosis/necrosis and DNA damage, while not causing loss of viability or reactive oxygen species (ROS) production, in human SHSY5Y neuron cells [18]. On the other hand, reports show that ≤50 nm TiO_2NPs could induce strong oxidative stress, lipid peroxidation, mitochondria disruption and damage, and apoptosis in human astrocytoma (U373) and rat microglia cells (C6) [19,20]. However, significantly less is known about the effects of TiO_2NPs in cell-cell interaction.

Cell-cell interaction plays a pivotal role in the development of neurodegenerative disease, such as Alzheimer's (AD) and Parkinson's disease (PD). For instance, in AD, production and deposition of amyloid-β (Aβ) have been shown to quickly increase intracellular Ca^{2+} in astrocytes, which leads to mitochondrial depolarization and ROS production, causing neuronal death in astrocyte-neuron interaction [21,22]. The Aβ also activated a nuclear factor-kappaB (NFκB) dependent pathway required for cytokine production. It also induced TNF-α release and led to iNOS-dependent neuronal apoptosis in microglia-neuron interaction [23]. In astrocytes-microglia interaction, Aβ-induced ATP release from astrocyte, which triggered TNF-α release from microglia, thus inducing a proliferation of migration of microglia towards the injury site [24,25].

Recent studies have found that either magnetic or silver NPs are taken up mainly by astrocytes or microglia, not by neurons [26,27]. Thus, effects of TiO_2NPs on microglia and astrocytes may play important roles in the toxic mechanisms of NPs in CNS, which strengthens the need to study their effects in neuron-glia interaction. So far, few studies have found that TiO_2NP-induced ROS or cytokine release from microglia might damage neurons [28,29]. However, almost none of the study reports discuss astrocyte-neuron and astrocyte-microglia interaction in the treatment of NPs.

Moreover, it is also essential to study cellular uptake mechanisms and lysosomal translocation of TiO_2NPs in the glia cells because the interaction between NPs and the lysosomal compartment has been regarded as an emerging mechanism for nanomaterial toxicity [30]. On the other hand, as microglia and astrocyte activation occur following almost all CNS pathologies, such as AD and PD, it is also crucial to understand if NP exposure promotes more serious responses under activated state.

In this study, we assumed that neurons could be damaged indirectly by soluble factors (NO, ROS, cytokines) in microglia or astrocytes through high amounts of TiO_2NP uptake by endocytosis pathways. Indirect effects could be enhanced in the activated state of glial cells. To confirm this hypothesis, toxic responses of 6 nm of 100% anatase TiO_2NPs to murine brain astrocyte-like (ALT), immortalized microglia (BV-2) and differentiated neuroblastoma (N2a) cells were studied. Cell viability, cell-death process (N2a), uptake, intracellular ROS, extracellular nitric oxide (NO) and H_2O_2, and cytokines (IL-1β, IL-6, TNF-α, and MCP-1) release in monoculture were first analyzed. The uptake mechanisms of TiO_2NPs and NP-lysosome co-localization in ALT, BV-2 and activated BV-2 were also studied. Indirect effects of TiO_2NPs on N2a or BV-2 were studied via ALT-N2a, BV-2-N2a and ALT-BV-2 co-culture using the Transwell® system. Cell viability of N2a, or BV-2, and cell-death process of N2a were used for identifying cell damage. Cell uptake, intracellular ROS and cytokines release in both chambers were analyzed. The effects of TiO_2NP in activated states of the three cell lines were investigated by co-administration of lipopolysaccharides (LPS).

2. Materials and methods

2.1. Nanoparticle source

Alkali-modified TiO_2NPs were synthesized in this study. The alkali modification process has been shown to increase the density of surface hydroxyl groups on the TiO_2, and then enhance the dispersion and photocatalytic activity [31]. First, 1 g of TiO_2 commercial nanopowder (ST-01, 100% anatase, Ishihara Corporation, Japan) was dispersed in a 100 mM H_2O_2 and 8 M NaOH mixed aqueous solution. The crystalline diameter of the nanopowder was 7 nm. Then, the suspension was heated to 50 °C and kept for 24 h. After centrifugation at 8000 rpm for 20 min, the particles were washed twice with de-ionized water and re-dispersed in a 1.6 M HNO_3 solution. The suspension was stirred for 3 h, and then centrifuged at 13,500 rpm for 20 min. After three washes with de-ionized water, the TiO_2NPs were dried at 60 °C and re-dispersed in water for subsequent experiments. Solutions had good stability in storage for at least six months at 4 °C.

2.2. Nanoparticle physicochemical characterization

Before characterizing NP in water or cell medium, TiO_2NP stock solution (4000 μg/mL) was first ultrasonicated at 400 W for 10 min (DC400H, DELTA New Instrument Ltd., Taiwan) at 25 °C to achieve optimal dispersion. The size and morphology of the NPs in stock solution were analyzed using a JEM2100 transmission electron microscope (TEM) (JEOL, Japan). The hydrodynamic size and surface charge of the NPs in water and cell medium (Dulbecco's Modified Eagle's Medium, DMEM) with HEPES and L-Glutamine (Gibco® Invitrogen, CA) supplemented with 10% Fetal Bovine Serum (FBS) (Biological Industries, Israel)] was monitored using a Zetasizer Nano ZS apparatus (Malvern Instruments, UK). For measurements, particles were diluted to 100–5 μg/mL. To observe the stability of NPs in cell media, variations in size after 24 h of incubation were monitored.

2.3. Monoculture, LPS treatment and TiO_2NP exposure

Murine brain astrocyte-like ALT (BCRC 60581, Taiwan), murine microglial BV-2 cells (ATL03001, ICLC, Genova, Italy) and murine neuroblastoma Neuro-2a (N2a) cells (BCRC 60026, Taiwan) were used in the study. N2a cells were cultured in high-glucose DMEM with L-Glutamine supplemented with 10% FBS, 1% penicillin-streptomycin (Biological Industries, Israel), and 1% sodium pyruvate (Invitrogen, CA). ALT cells and BV-2 cells were cultured in the same medium as N2a cells, but without 1% sodium pyruvate. For differentiation, N2a cells were treated with 30 μM forskolin and 200 μM isobutylmethylxanthine (IBMX) (Sigma-Aldrich, St. Louis, MO, USA) in DMEM supplemented with 1% FBS for 2 days after 1 day of attachment [32]. Three cell lines were cultivated at 37 °C, 5% CO_2 and 95% relative humidity.

Cells were seeded and attached for 24 h (9×10^3 cells/cm^2 for ALT and BV-2; 5×10^3 cells/cm^2 for N2a). To induce inflammation responses prior to NP treatment, cells were pre-treated with LPS from *Escherichia coli* 055:B5 (Sigma-Aldrich, St. Louis, MO, USA)(0.2 μg/mL for BV-2 cells and 2 μg/mL for ALT and N2a cells) in serum-free DMEM medium for 6 h. For non-LPS group, cells were incubated only in serum-free medium. TiO_2NPs were first diluted to an indicated concentration (200–10 μg/mL) in DMEM/20%FBS, and then the same volume of NP suspensions as pre-treatment use were added to achieve final concentration of LPS (0.1 μg/mL for BV-2 cells and 1 μg/mL for ALT and N2a cells) and TiO_2NPs (100–5 μg/mL) in DMEM/10%FBS medium.

2.4. Co-culture, LPS treatment and TiO_2NP exposure

For co-culture of ALT and N2a/BV-2 and N2a, N2a cells (5×10^3 cells/cm^2) were first seeded in the upper chamber (insert) of 24-well or 6-well Transwell plates (0.4 μm pore size, polyester

membrane) (Corning Inc. MA, USA)). After 24 h of attachment, cells were differentiated by forskolin and IBMX for 2 days. On the third day, ALT cells (9×10^3 cells/cm^2) or BV-2 cells (1.6×10^3 cells/cm^2) were seeded in separate 24-well or 6-well plates. After 24 h of attachment, the inserts and culture plates which contained differentiated N2a cells and ALT or BV-2, respectively, were combined before following LPS or NP exposure. For ALT and BV-2 co-culture, BV-2 cells (1×10^4 cells/cm^2) and ALT (9×10^3 cells/cm^2) were seeded separately in upper and bottom chambers of the Transwell, respectively. After 24 h of attachment, the inserts and culture plates were combined together before following up with LPS or NP exposure. Cell density for the three co-cultured systems was determined by the ratio between the initial number of seeding cells which should be equal to 10% neuron, 9–18% microglia, and 72–81% astrocytes, and which corresponds to the cell ratio in a human brain [33,34]. To induce inflammation responses prior to NP treatment, bottom chamber cells were pre-treated with LPS (0.2 μg/mL for BV-2-N2a and ALT-BV-2 and 2 μg/mL for ALT-N2a co-culture system) in serum-free DMEM medium for 6 h. For the non-LPS group, cells were incubated only in a serum-free medium. Then, the same volume of NP suspensions for pre-treatment use were added to achieve final concentrations of LPS (0.1 μg/mL for BV-2-N2a and ALT-BV-2 co-culture system and 1 μg/mL for ALT-N2a co-culture system) and TiO_2NPs (100 and 30 μg/mL) in DMEM/10%FBS medium in bottom chamber. In inserts, an equal volume of fresh DMEM/20%FBS as serum-free medium was added.

2.5. Cell viability

After 24 and 48 h of TiO_2NP exposure, all NP suspensions were discarded and alamarBlue® (AbD Serotec, Kidlington, UK) was added. Briefly, the alamarBlue® reagent was mixed 1:10 with fresh DMEM/10%FBS, followed by a 1.5 h incubation at 37 °C. For co-culture system, cells in insert and bottom chambers were incubated 1.5 h separately in alamarBlue/DMEM/10%FBS mixture (e.g., inserts were moved into fresh well plates). Results were evaluated by monitoring fluorescence at excitation wavelengths of 530 nm with emissions at 590 nm using a top reading mode (Synergy HT, BioTek, USA). The top reading mode prevented signal collection from adherent cells, which minimized interference from intracellular NP. Cell viability was calculated using the expression (fluorescence intensity (FI) of test sample-FI of reagent blank)/(FI of untreated control-FI of reagent blank) × 100.

2.6. Cell death process of N2a

Cell death process was evaluated for direct and indirect effects of TiO_2NPs on differentiated N2a cells. For direct exposure, N2a cells (5×10^3 cells/cm^2) were seeded in 6-well culture plates. For indirect exposure, the co-culture groups of ALT-N2a and BV-2-N2a were prepared based on above-mentioned procedures. Live, necrotic, early- and late-apoptotic cells were distinguished using an Annexin V-FITC/propidium iodide (PI) assay kit (biotool.com, Houston, TX, USA). Sample preparation was conducted according to the manufacturer's protocol. Fluorescence channel FITC and PerCP-Cy5.5 were used to detect Annexin V and PI in BD FACSCanto II flow cytometer (BD Biosciences, San Jose, CA, USA), with 10,000 cells collected. Data was analyzed using Flowing Software 2.

2.7. NP uptake potential and quantification

Uptake potential of TiO_2NPs was measured by flow cytometry light-scatter analysis developed by Suzuki et al. [35]. After 24 h of NP exposure, suspensions were removed and the cells were rinsed three times with phosphate-buffered saline (PBS). Next, the cells were harvested. Evaluation of geometric mean SSC intensity was carried out using a FACSCanto II, and data were analyzed using Flowing Software 2. Data was calculated using the expression (SSC intensity of test sample)/(SSC intensity of untreated control or LPS-only treated control) × 100.

2.8. Intracellular ROS

Production of H_2O_2, a major intracellular ROS, was measured using 2′,7′-dichlorofluorescin diacetate (DCFH-DA, Sigma-Aldrich, MO, USA) as a reactive fluorescent probe. The intracellular ROS and uptake potential could be measured simultaneously [36]. The DCFH-DA working solution, obtained after diluting 20 mM DCFH-DA of stock solution (in methanol) to 10 μM in serum and phenol red-free DMEM, was added to each collected cell, followed by incubation for 30 min at 37 °C. The solution was then centrifuged (200*g*, 5 min) and the supernatant was removed. Prior to measurement, the cells were re-suspended in PBS. Then 2 mM of H_2O_2 were treated for 15 min before the end of NP exposure as a positive control. Fluorescence was determined at 528 nm after excitation at 488 nm using a FACSCanto II flow cytometer, with 10,000 cells collected. Data was analyzed using Flowing Software 2. About 50% of cell total that had higher fluorescence intensity in the control sample were gated by histogram analysis. Any increased or decreased distribution of fluorescence intensity from other samples would get a higher or lower percentage of cells within the gating range.

2.9. Extracellular NO and H_2O_2

Cells (1×10^4 cells/cm^2 for ALT and BV-2) were first seeded in 24-well plates. After 4 and 24 h TiO_2NP exposure, the 0.5 mL suspensions were collected. To avoid interference, most of the serum in suspensions was removed using 10 kDa molecular weight cut-off filters (Pall Corp., NY, USA) with 14,000 g centrifugal force at 4 °C. Then, aliquot of samples (20 μL for Nitrite assay; 5 μL for H_2O_2 assay) were used based on the manufacturer's protocols (Nitrate/Nitrite fluorometric assay kit, Cayman Chemical Company, MI; Hydrogen peroxide fluorescent detection kit, Arbor Assays, MI, USA). After performing the assays, results were evaluated by monitoring fluorescence at an excitation wavelength of 360 nm with emission at 430 nm for nitrite assay, and an excitation wavelength of 560 nm with emission at 590 nm for hydrogen peroxide assay.

2.10. Chemokine/cytokine detection

Supernatants, which were collected from well plates (monoculture) or from bottom and upper Transwell chambers (co-culture) were used for cytokine measurement. They were stored in −80 °C until used. Pro-inflammatory mediators IL-1β, IL-6, TNF-α, and MCP-1 were measured by a commercially available ELISA Development Kit (eBioscience, Inc. CA, USA) according to the manufacturer's protocol.

2.11. Uptake mechanisms

For endocytic pathway inhibition experiments, ALT, BV-2, and LPS-activated BV-2 cells were pre-incubated for 30 min with different inhibitors at the following concentrations: genistein (100 μM), filipin III (1.5 μM for ALT; 7.5 μM for BV-2), amiloride hydrochloride (100 μM), chlorpromazine hydrochloride (CPZ) (14 μM), monodansylcadaverine (MDC) (75 μM) and phenylarsine oxide (PAO) (0.006 μM for ALT; 0.3 μM for BV-2) (all from Sigma-Aldrich, St. Louis, MO, USA). TiO_2NPs were then added and

incubated for 1.5 h. After exposure, the suspensions were discarded and cells were washed twice with PBS. Finally, cells were trypsinized and harvested. To count the cell concentration, 10 μL of suspension was taken from harvested cells. After centrifugation (250g, 5 min), supernatant was discarded and the cell pellet was acidified with 1 mL HNO_3, plus 2 mL 5%HF. Suspensions were then digested at 70 °C for 24 h and filled to 15 mL with 10 ppb of Y as internal standard before analysis. ^{47}Ti and ^{89}Y analysis was conducted using a quadrupole ICP-MS (Agilent 7500a, USA). Prior to the experiment, we had analyzed the cytotoxicity of the inhibitors after 2.5 h by alamarBlue® and used only sub-cytotoxic doses (cell viability higher than 80%) (data not shown). BODIPY-LacCer (lactosylceramide complexed to BSA, 0.5 μM) (for Genistein and Filipin), Transferrin-Alexa Fluor 488 (0.25 μg/mL) (for CPZ and MDC) and Dextran-Oregon Green 488; 70,000 MW (12 μg/mL) (for Amiloride and PAO) (all from Life Technologies, CA, USA) were used as control substrates to measure the efficiency of inhibitors. The inhibitors were pre-incubated for 30 min, and then the substrate was added and incubated for 2 h. Fluorescence was determined at 528 nm after excitation at 488 nm using a FACSCanto II flow cytometer, with 10,000 cells collected.

2.12. Lysosome tracking

Cells were treated with TiO_2NP (25 μg/mL) suspensions for 8, 16, and 24 h after seeding 5.2×10^3 cells/cm^2 on coverslips in 12-well culture plates. After incubation, 500 nM LysoTracker Green DND-26 (Life Technologies, CA, USA) was added and incubated at 37 °C for 10 min (for ALT) or 20 min (for BV-2 and LPS-activated BV-2). Cells were washed with PBS three times, then fixed with 4% paraformaldehyde (PFA) in PBS for 20 min at room temperature. Coverslips were covered by ProLong® antifade mountant with 4′,6-diamidino-2-phenylindole (DAPI) (Life Technologies, CA, USA) for nuclei staining. Images were obtained from the combination of fluorescence and dark field microscopy with 60 × Plan Fluor with an iris diaphragm (Nikon Ti–U series microscopy, Japan).

2.13. Quantifying TiO_2NPs in cells after direct or indirect exposure

Cells (5×10^3 cells/cm^2 for N2a; 1×10^4 cells/cm^2 for BV-2) were seeded in the insert of 6-well Transwell plates (indirect exposure) or 6-well plates (direct exposure). After attachment and differentiation, cells were incubated in serum-free medium for 6 h. Then, a final concentration of TiO_2NPs (100 μg/mL) was added in the lower chamber of Transwell plates, or culture plates, and incubated for 24 h. The NP suspensions were then discarded and cells were washed with PBS three times. Procedures for ICP-MS quantification of NPs in cells were the same as in the uptake mechanisms study (2.11).

2.14. Statistics

Significant differences between control/LPS-only group and treatment groups were analyzed in GraphPad Prism (version 5.02) by one-way analysis of variance (ANOVA) followed by Dunnett's multiple comparison post-tests. For two-group comparison, Student's unpaired t–test was used. $p < 0.05$ was considered statistically significant.

3. Results

3.1. NP physicochemical characterization

From TEM images, the geometric mean primary size of TiO_2NPs was 5.8 nm, while they formed several agglomerates with sizes between 30 and 60 nm (Fig. S1). Dynamic laser scattering (DLS) measurement showed that TiO_2NPs was 44.4 and 92 nm in water and culture medium respectively, and had good stability after 24 h (Table 1, Figs. 1 and S2). TiO_2NP particles had a positive surface charge (zeta potential) in water and negative charge in cell media (Table 1). The positive charge of alkali-modified TiO_2NPs in water is mainly due to remaining acid (HNO_3) in stock solution. On one hand, the initial DLS sizes of TiO_2NPs decreased with the decrement of concentration (Fig. 1), which might be explained by different ratios between TiO_2NPs and DMEM/10%FBS medium.

3.2. Direct effects: cytotoxicity of TiO_2NPs

Fig. 2A shows the cell viability of ALT, BV-2 and differentiated N2a cells after 24 h exposure. TiO_2NPs had a dose- and cell type-dependent toxicity. They caused the highest cytotoxicity on ALT, followed by BV-2, and the least on differentiated N2a. Uptake potential was then analyzed by flow cytometry. The uptake profiles were clearly dose- and cell dependent (Fig. 2B). ALT and BV-2 took up similar amounts of TiO_2NPs, and were higher than that in N2a. The intracellular ROS of three cell lines were measured using the DCFH-DA assay. ROS was significantly induced in ALT and BV-2 at 100 μg/mL after 24 h (Fig. 2C), while not induced in the three cell lines after 4 h (Fig. S3). No ROS was induced in N2a after 4 or 24 h of exposure (Fig. 2C, S3). The cell viability correlated well with the ROS production in the three cell types. IL-1β, IL-6, TNF-α, and MCP-1 were selected as inflammation markers because these mediators play a major role in prevention, but also enhance brain damage. TiO_2NPs induced IL-1β from all three cell lines and IL-6 from N2a cells (Fig. 3A, B).

Treatment of LPS caused mild toxicity in ALT (85%) and BV-2 (74%) cells, while not showing toxicity in N2a (Fig. 2A). After co-treatment of TiO_2NPs with LPS for 24 h, the cell viabilities were similar to NP-only treatment groups on ALT and N2a. Compared with the LPS-only group, no significant decrease of cell viability was found in BV-2 when co-treated with LPS and TiO_2NPs (Fig. 2A). On the other hand, LPS-activated BV-2 cells took up larger amounts of TiO_2NPs than normal BV-2 cells, while there were no differences in NP uptake between LPS-treated and un-treated ALT and N2a cells (Fig. 2B). LPS induced intracellular ROS in BV-2 after 24 h, and was more enhanced after co-treatment with TiO_2NPs (Fig. 2C). Similar synergetic results could be found in the 4 h data (Fig. S3). LPS induced IL-6 in BV-2 and N2a, TNF-α in BV-2, and MCP-1 release in ALT and BV-2 (Fig. 3A–C, S4). Moreover, the induction was enhanced after co-treatment with TiO_2NPs in N2a (IL-1β), ALT (IL-1β) and BV-2 (IL-1β, IL-6 and MCP-1) (Fig. 3A–C), which especially correlated well with above-mentioned ROS release results in BV-2 (Fig. 2C).

3.3. Direct effects: cell death progress of differentiated N2a

The cell death progress of neurons was measured because the apoptosis cascades are involved in Alzheimer's disease and other human neurological disorders [37]. The cell death process of differentiated N2a cells after direct TiO_2NP exposure for 24 h was detected by Annexin V/PI staining. The results are shown in Fig. 4. TiO_2NPs or TiO_2NP-LPS induced late apoptosis and decreased viable

Table 1
Hydrodynamic diameters (Z-Average) and surface charges of TiO_2NPs in water and DMEM/10%FBS at 0 h incubation (Concentration of TiO_2NPs: 100 μg/mL).

Samples	Media	DLS size (nm)	pdI	Zeta potential (mV)
TiO_2NPs	Water	44.4 ± 0.2	0.15	47.1
	DMEM/FBS	91.5 ± 2.3	0.60	−14.4

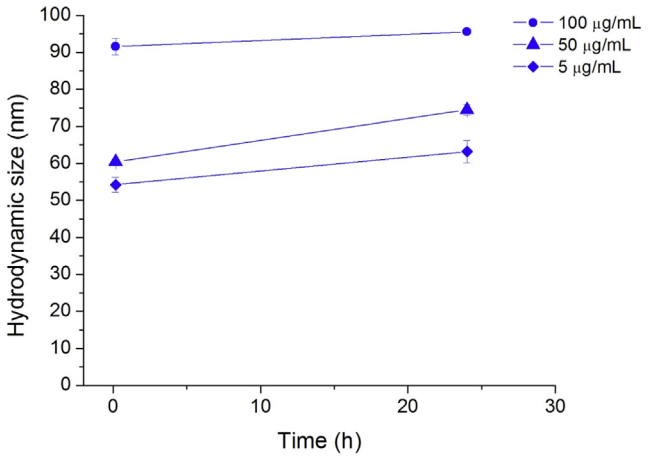

Fig. 1. Stability of TiO_2NPs in DMEM/10%FBS. Dynamic light scattering measurements were done at 0 and 24 h for AgNPs in different NP concentrations. The hydrodynamic size (Z-Ave) decreased with the decrement of the NP concentration.

cells of differentiated N2a cells. No significant difference was observed between LPS-only and control groups.

3.4. Direct effects: uptake mechanisms and lysosome trafficking in ALT and BV-2

Since TiO_2NPs were mainly taken up by astrocyte-like cells, microglia and LPS-activated microglia, we studied the mechanisms of NP uptake in those cells. This could be helpful to predict the portion and velocity at which NPs can enter into lysosome, an important place to trigger ROS. General active uptake mechanisms, including clathrin-dependent, caveolae-dependent endocytosis, macropinocytosis and phagocytosis were considered. Inhibitors genistein, filipin (for caveoleo-dependent), chlorpromazine, MDC (for clathrin-dependent), amiloride (for micropinocytosis) and PAO (for phagocytosis/clathrin-dependent endocytosis) were used. We have analyzed the efficiency of these inhibitors in our cell systems by using transferrin (clathrin-dependent), lactosylceramide (LacCer) (caveoleo-dependent) and dextran-70000 MW (for the other two pathways) as substrates [38,39] (data not shown). Fig. 5 shows analysis of uptake mechanisms of TiO_2NPs using different inhibitors. Genistein and MDC could decrease the uptake of TiO_2NPs in ALT, which blocked caveolae and clathrin-mediated endocytosis (Fig. 5A). Moreover, chlorpromazine and PAO inhibited the uptake of TiO_2NPs in BV-2, which blocked clathrin-dependent and phagocytosis pathways (Fig. 5B). Genistein, chlorpromazine, MDC and PAO decreased the uptake of TiO_2NPs in LPS-activated BV-2, which means all pathways were involved except micropinocytosis (Fig. 3C).

Whether or not TiO_2NPs translocate into lysosome relates to its toxicity. One reason is that NPs may induce ROS from lysosome, which is a major source of cellular ROS release [40]. To elucidate intracellular tracking of NPs, we investigated co-localization of internalized TiO_2NPs with Lysotracker Green which stains acidic compartments, such as late endosomes and lysosomes. To view NPs, we used dark-field microscopy [41]. A high co-localization between TiO_2NPs and lysosomes could be observed only after 16 and 24 h for ALT, BV-2 and LPS-activated BV-2 (Fig. 6); not after 8 h of exposure (data not shown).

3.5. Direct effects: extracellular H_2O_2 and NO production from ALT and BV-2

Here, extracellular H_2O_2 and nitrite released from BV-2 and ALT

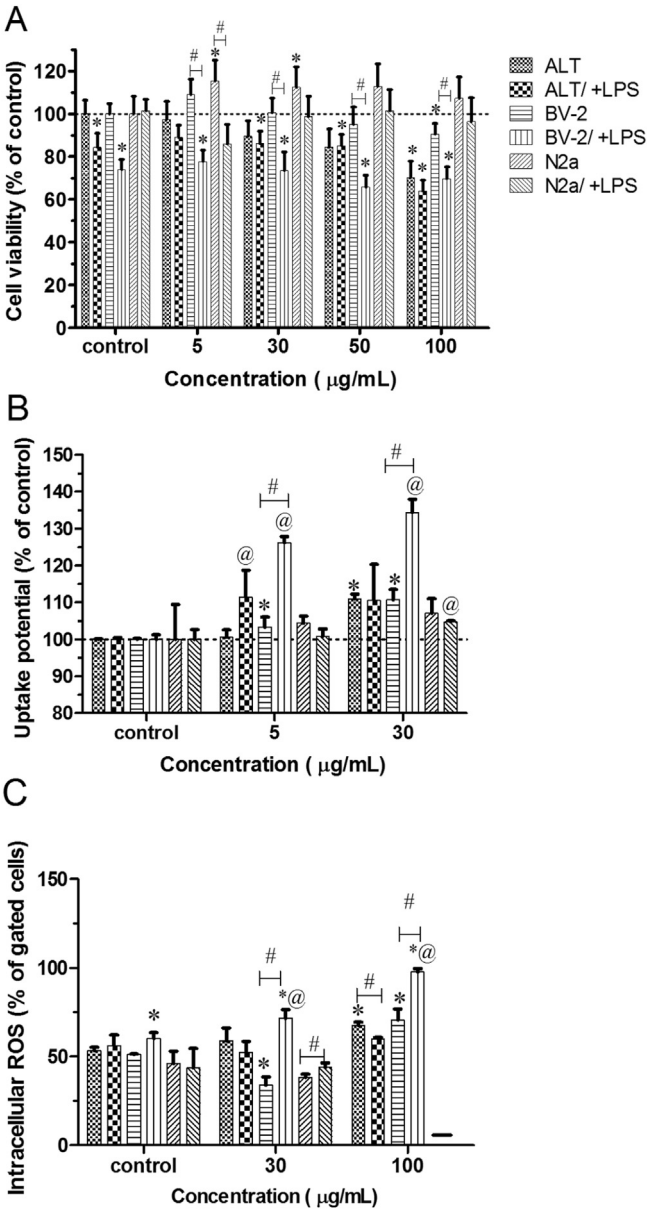

Fig. 2. Direct effects of TiO_2NPs with (+) or without LPS co-treatment in ALT, BV-2 and differentiated N2a cells after 24 h. (A) cell viability; (B) uptake potential; (C) intracellular ROS release. Data are presented as means ± SD (for cell viability n = 4; for others n = 3). (*) Significantly different from the control group. (@) Significantly different from the LPS-only treatment group. (#) Significantly different between two treatment groups.

were measured. After 24 h, BV-2 cells released significant amounts of H_2O_2 in response to the presence of TiO_2NPs (Fig. 7A). After 4 and 24 h, LPS-activated BV-2 cells released significant H_2O_2 into medium, and co-treatment of TiO_2NPs enhanced the release (Figs. S5 and 7). LPS-activated microglia released significant NO into medium, but co-treatment with TiO_2NPs did not change the release level (Fig. 7B). The results suggest that TiO_2NPs might induce either extracellular H_2O_2 release from BV-2 or LPS-activated BV-2, and indirectly damage N2a cells.

3.6. Indirect effects: cytotoxicity of TiO_2NPs to N2a in ALT-N2a and BV-2-N2a co-culture

To confirm the above-mentioned hypothesis, a co-culture

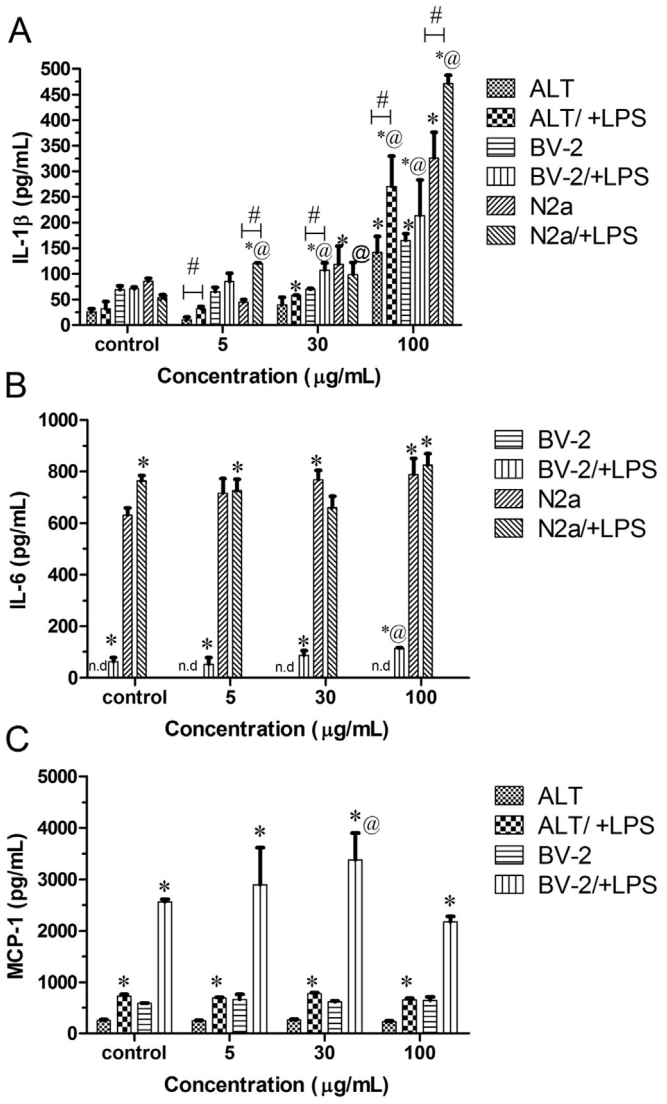

Fig. 3. Direct effects of TiO_2NPs with (+) or without LPS co-treatment in ALT, BV-2 and differentiated N2a cells after 24 h. (A) IL-1β; (B) IL-6; (C) MCP-1 release. Data are presented as means ± SD (n = 3). (*) Significantly different from the control group. (@) Significantly different from the LPS-only treatment group. (#) Significantly different between two treatment groups. n.d.: not detected.

experiment between ALT/BV-2 and N2a was conducted using Transwell system. Basically, three types of co-cultured systems were used frequently: (1) a conditioned medium-transfer system (2) a direct co-culture system allowing cell-cell contact and communication, and (3) a Transwell® system, which allows communication through diffusible and soluble factors with no cell contact [42]. We selected the Transwell system not only because it allows cell-cell simultaneous interaction, thus avoiding loss of short half-life species, such as ROS, when using a conditioned medium transfer system, but it also distinguishes the effects on different kinds of cells after TiO_2NP exposure. To demonstrate the indirect TiO_2NP effects on N2a cells, it is essential to prove significantly less uptake of TiO_2NPs in the N2a cells of the Transwell system, which minimized direct NP effects. We thus compared the amount of TiO_2NPs in each N2a cell between direct and indirect exposure at the same concentration by ICP-MS (Fig. S6A). The indirect exposure showed only 23.5% of Ti compared with direct exposure in N2a (Fig. S6B). Indirect exposure of 100 μg/mL TiO_2NPs to ALT or BV-2 did not induce more early- or late-apoptotic N2a cells (Fig. 8). However, indirect exposure of TiO_2NPs with LPS induced more late apoptotic N2a cells in BV-2-N2a co-culture (Fig. 8), which was more serious than the LPS-only effects on the N2a in the same co-culture system (early apoptosis). Corresponding to the cell death process, viability of N2a was not affected after indirect TiO_2NP exposure in ALT-N2a co-culture (Fig. S7A). The intracellular ROS was even inhibited in N2a cells for both TiO_2NP and TiO_2NP-LPS co-treatment groups (Fig. S7B). TiO_2NPs inhibited IL-6, but induced MCP-1 release in both ALT and N2a supernatant (Fig. S7E, G). However, there was no further secretion of both cytokines for TiO_2NP-LPS co-treatment groups. On the other hand, viability of N2a decreased significantly to 58% and 64% when the TiO_2NPs were co-treated with LPS to BV-2 at 30 and 100 μg/mL (Fig. S7B), which also corresponds to the cell death progression results. In addition, intracellular ROS were induced in both BV-2 and N2a cells for TiO_2NP-LPS co-treatment groups (Fig. S7D). IL-6, MCP-1 and TNF-α release in supernatant of both chambers were also induced and enhanced for TiO_2NP-LPS co-treatment groups (Fig. S7F, H, I).

3.7. Indirect effects: cytotoxicity of TiO_2NPs to BV-2 in ALT-BV-2 co-culture

In addition to indirect effects of TiO_2NPs on N2a, we also investigated their indirect effects on BV-2 cells in a co-culture of ALT cells. The amount of Ti in each BV-2 cell for direct and indirect exposure was compared (Fig. S6). Indirect exposure showed only 9.1% of Ti compared to direct exposure in each BV-2 (Fig. S6B). Indirect exposure of TiO_2NPs or TiO_2NP-LPS did not cause any further toxicity to microglia (Fig. S8A). Corresponding to the cell viability results, no ROS could be induced (Fig. S8B). Figs. S8C–E show the level of IL-6, TNF-α and MCP-1 in the ALT- and BV-2-containing chambers' supernatants. Only indirect exposure of 30 μg/mL TiO_2NPs with LPS induced more TNF-α release in the chambers containing BV-2 (Fig. S8D).

4. Discussion

4.1. Astrocytes and microglia are more susceptible than neurons to TiO_2NPs

In our study, 6 nm of TiO_2NPs caused the highest cytotoxicity on astrocyte-like cells, followed by microglia, and the least on neuron-like cells, which correlated well with uptake and intracellular/extracellular ROS release results. Similar to our study, degussa P25 TiO_2NPs caused neurotoxicity and stimulation of ROS in BV-2 while showing nontoxicity to isolated N27 neurons [29]. In a mixed neuron and astrocyte cell model, Haase et al. found that astrocytes took up much more 20 nm peptide-coated AgNPs compared with neurons, and also more vulnerable to NPs than neurons [27]. Generation of ROS also was found in mixed primary cortical cell in the same report. Astrocytes and microglia account for about 90% in CNS system. Astrocytes are found in the BBB, and are more easily exposed to NPs than other brain cells. Thus, our findings suggest that toxic mechanisms of NPs in CNS may arise from glia cells, not neurons.

4.2. Activated microglia take up large amounts of TiO_2NPs and induce more ROS

Most studies have examined the uptake and toxicity of activated microglia on magnetic NPs because they have a wide application as magnetic resonance imaging contrast agents [43,44]. One report indicates that LPS-mediated stimulation of magnetic NP uptake was transient, and might be more related to early steps in the activation

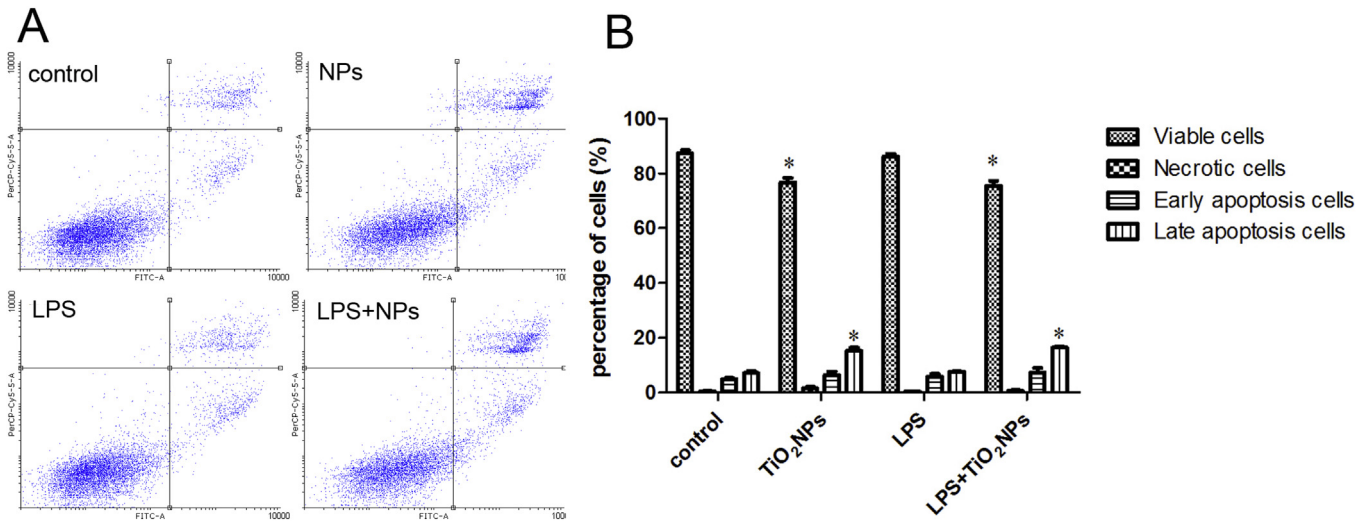

Fig. 4. Effect of TiO_2NPs on the progressive apoptosis of neurons. Representative dot plots of Annexin V/PI staining are shown in (A). The upper-left quadrant shows the necrotic population. The upper-right quadrant shows the late apoptotic. The lower-left quadrant shows the live-cell population. The lower-right quadrant shows the early apoptotic population. (B) The percentage of viable cells, early apoptotic cells, late apoptotic cells and necrotic cells after being exposed to 100 μg/mL TiO_2NPs for 24 h. Data are presented as means ± SD (n = 3). (*) Significantly different from the control group.

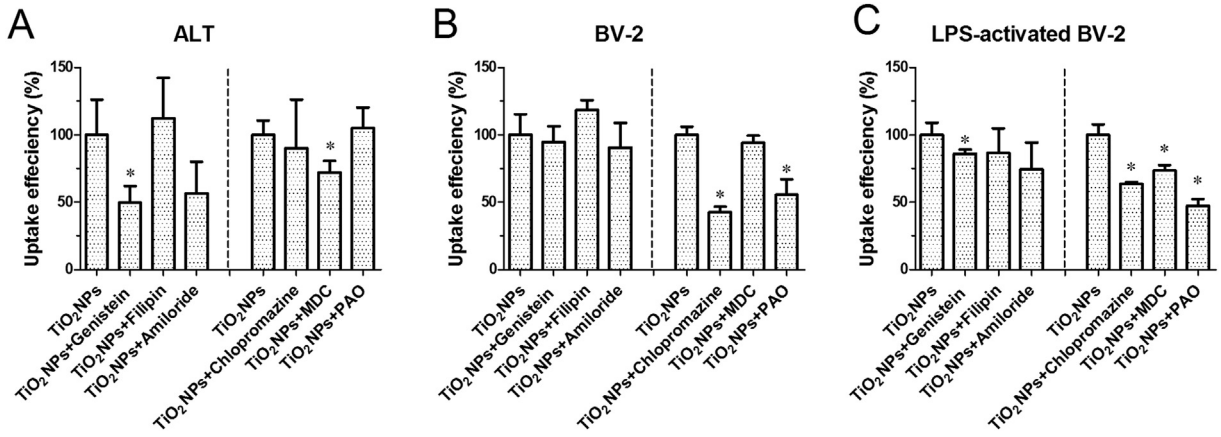

Fig. 5. Analysis of uptake mechanisms of TiO_2NPs using different inhibitors. Cells were pretreated with various inhibitors (Genistein, Filipin, Chlorpromazine, MDC, Amiloride and PAO) for 30 min, followed by exposure to TiO_2NPs (50 μg/mL) in (A) ALT, (B) BV-2 and (C) LPS-activated BV-2 for 2 h. The data was measured by ICP-MS with normalization of cell numbers. Data are presented as means ± SD (n = 3). (*) Significantly different from the control group (TiO_2NPs treatment without inhibitors).

process [26]. This study found that LPS-activated microglia were induced to take up more TiO_2NPs when pretreated with LPS for short times (6 h) followed by NP exposure for 24 h, which supports the suggestion. On the other hand, the synergetic ROS induction of TiO_2NPs in LPS-activated BV-2 may be explained by a higher amount of NP uptake than normal BV-2 and/or a greater uptake of LPS due to adsorption of LPS on NP surface [45]. This suggests that when the brain has been injured, NP exposure may cause sustained oxidative stress in activated microglia and finally damage the neurons.

4.3. TiO_2NPs were able to induce cytokines release, especially when co-treated with LPS

In monoculture study, TiO_2NPs were able to induce IL-1β in all cell lines and IL-6 in N2a. In addition, co-treatment of LPS induced more IL-1β in all cell lines, IL-6 and MCP-1 in BV-2 cells, which indicated a synergistic cytokine release on TiO_2NP-LPS co-treatment group. In BV-2-N2a and ALT-BV-2 co-culture, TiO_2NPs were also able to induce more TNF-α from LPS-activated BV-2. In agreement with our study, TiO_2NPs induced IL-1β, TNF-α and IL-10 release in rat astrocyte [17], TNF-α, IL-1β, IL-6 release [28], and gene expression of MCP-1, MIP-1α in rat primary microglia, and up-regulated inflammation genes (NF-κ B, IL-1, etc.) in BV-2 microglia [29]. The synergistic inflammatory effect of TiO_2NPs and LPS in CNS has not been reported. However, one study found enhanced inflammatory responses of macrophage in TiO_2-LPS co-treatment through a TLR4-dependent intracellular pathway. This finding supports our results [45]. Transcription factor NF-κB activity is regulated by intracellular ROS, which then mediates release of pro-inflammatory cytokines (IL-1β, IL-6, MCP-1, TNF-α) [46]. IL-1β emission also was enabled through ROS-mediated NLRP3 inflammasome activation [47]. The induction of cytokine release correlated well with intracellular or extracellular ROS production in BV-2 and ALT, which indicates ROS is a major factor in mediating inflammatory responses in astrocytes and microglia. These cytokines play a major role in preventing, but also enhancing brain damage. IL-1β release from microglia can activate astrocytes, promoting the

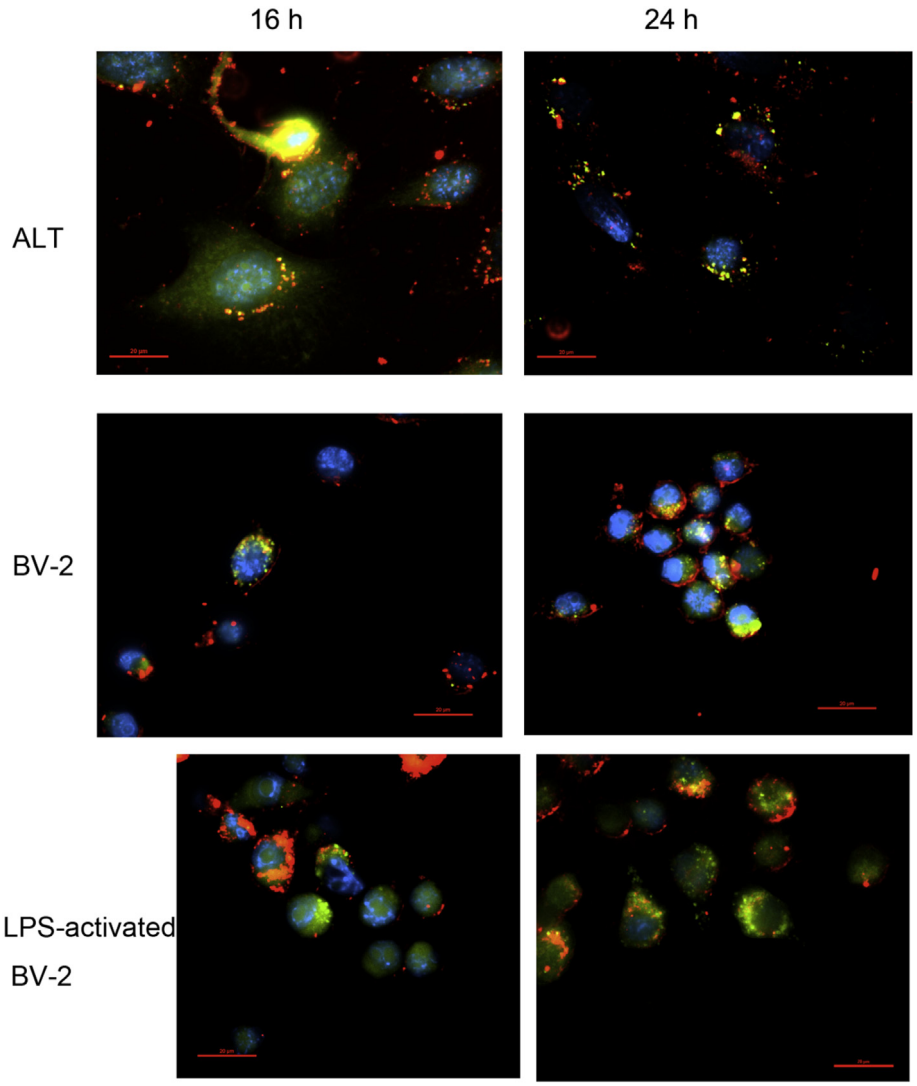

Fig. 6. Co-localization of TiO_2NPs and lysosomes after 16 and 24 h exposure. NPs are depicted in red, lysosomes are stained in green using Lysotracker Green, and nuclei are depicted in blue using DAPI. Co-localization of NPs and lysosomes is indicated by yellow color in the merged image resulting from overlaying green and red colors. Scale bar = 20 μm.

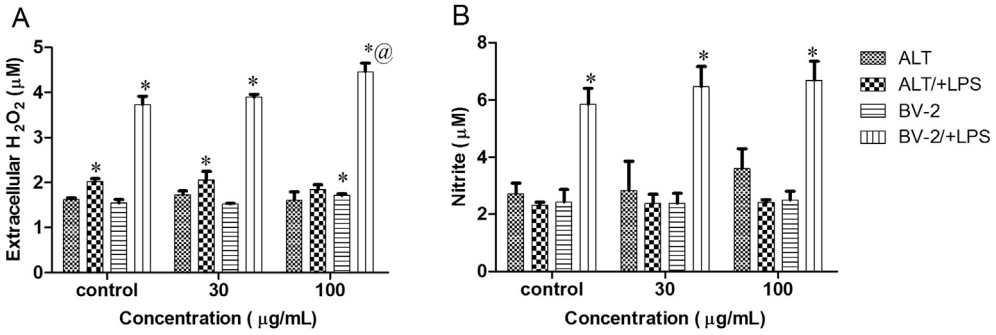

Fig. 7. Extracellular release of (A) H_2O_2 and (B) NO from ALT and BV-2 after treatment with TiO_2NPs with (+) or without LPS co-treatment for 24 h. Data are presented as means ± SD (n = 3). (*) Significantly different from the control group. (@) Significantly different from the LPS-only treatment group.

repair of CNS [48]. In mild amounts, IL-6 enhances the differentiation and survival of neuron cells [49]. IL-6 has also been found to have neuroprotective effects in neurons exposed to glutamate excitotoxicity [50,51]. MCP-1, one of the chemokines, serves to regulate microglial movement, and protect human neurons and astrocyte damage against different stimuli. TNF-α can stimulate survival and proliferation of neuron cells, and induce glutamate release from astrocytes [52]. However, high and sustained release

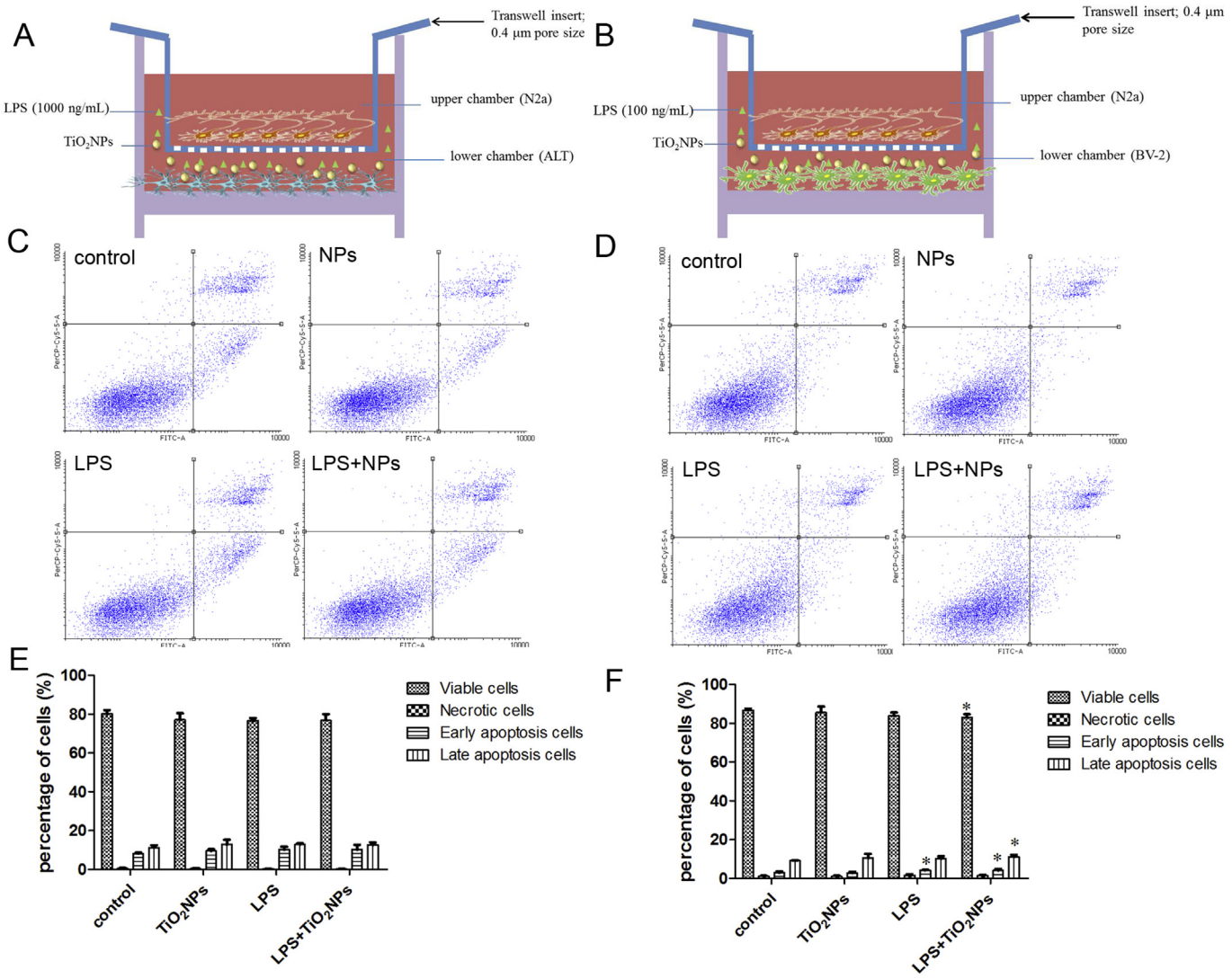

Fig. 8. Effect of indirect TiO_2NPs exposure on the progressive apoptosis of N2a. (A) ALT-N2a co-culture; (B) BV-2-N2a co-culture. Representative dot plots of Annexin V/PI staining are shown in (C) for ALT-N2a and (D) for BV-2-N2a. (E) (F) The corresponding percentage of viable cells, early apoptotic cells, late apoptotic cells and necrotic cells after being exposed to TiO_2NPs for 24 h. Data are presented as means ± SD (n = 3). (*) Significantly different from the control group.

of TNF-α can cause neuron damage [53]. Thus, the contribution of NP-induced cytokines release on the survival and functionality of neuron and glial cells should be further studied.

4.4. Uptake mechanism of TiO_2NPs is cell-type dependent, but NPs can translocate to the lysosome of both glia cells

In brain, phagocytosis occurs mainly in microglia and is enhanced in activated state [54]. Our study also found that some TiO_2NPs were taken up by phagocytosis in BV-2 and LPS-activated BV-2. In addition, activated BV-2 was involved in more uptake mechanisms for engulfing NPs than normal BV-2 and ALT cells. This can be expected, because the activated microglia act with macrophage-like functions. In addition, uptake mechanisms of TiO_2NPs differed between ALT, BV-2 and LPS-activated BV-2. This demonstrated cell type-dependent uptake mechanisms.

Uptake mechanisms of NPs would determine whether they could be translocated into lysosome. In phagocytosis, formation of phagosome vesicles will fuse with lysosomes within a few minutes [55]. The translocation of NPs into lysosome via the pathway of clathrin-mediated endocytosis primarily needs a few hours. Caveolae-mediated endocytosis was the only pathway in this study that could bypass lysosomes. Therefore, we could expect that TiO_2NPs can finally enter into lysosomes of all kinds of cells we tested, because at least one lysosome-related uptake mechanism was involved. Corresponding to our expectation, we found high co-localization of TiO_2NPs and lysosome in the three cells (Fig. 6). However, the translocation rate of NP to lysosome was slow (after 16 h) (Fig. 2). This may explain a slow intra/extracellular ROS production (after 24 h, not in 4 h) from ALT and BV-2.

4.5. TiO_2NPs can damage N2a cells indirectly by H_2O_2 and/or TNF-α release from LPS-activated BV-2 cells

It is known that LPS can activate microglia, release soluble factors, such as IL-6, TNF-α, nitric oxide and ROS, and then destroy neurons [56]. In this study, LPS treatment (1 μg/mL) to N2a did not lead to more early/late apoptosis of cells (Fig. 4B). However, treatment of low-concentrated LPS (0.1 μg/mL) in BV-2-N2a co-culturing caused more early apoptotic N2a cells, which could be attributed to the release of soluble factors [extracellular H_2O_2 (3.7 μM), NO (5.8 μM), and TNF-α (15 pg/mL)] from BV-2 (Fig. 7) and served as a

good positive control in the BV-2-N2a co-culture experiments. Our BV-2-N2a co-culture study indicated that increased late apoptotic and decreased viable N2a in indirect co-treatment of TiO_2NPs, and LPS could be mediated by BV-2. This may be explained by more H_2O_2 release (4.5 μM) and/or TNF-α (20 pg/mL) from LPS-activated BV-2 because previous studies have found H_2O_2-induced or TNF-α-mediated apoptosis in neuron cells [57,58]. On the other hand, without LPS-pretreatment, even though H_2O_2 (1.7 μM) was induced from BV-2 when treated with TiO_2NPs in the BV-2-N2a co-culture, no toxic effects on N2a cells were observed. This could be explained by low H_2O_2 and no NO or cytokine release from BV-2. Unlike a previous study using 20–45 nm TiO_2 [28], our study did not find that TiO_2NP-mediated NO production from microglia could damage neuron cells, which presumably is because we used a lower dose (0.1 mg/mL) than that used, according to that study's report (0.5 mg/mL).

Neither N2a nor BV-2 was affected by indirect TiO_2NPs or TiO_2NP-LPS exposure to ALT-N2a or ALT-BV-2 co-culture, which suggests that indirect neuron damage would not mainly arise from TiO_2NP-astrocyte interaction. Finally, more TNF-α was detected in BV-2 in the co-treatment of TiO_2NPs and LPS in ALT-BV-2, which presumably is triggered by ATP release from astrocyte [25,59]. Although the induction of TNF-α was not high enough to toxic microglia, it may induce proliferation of microglia as a protection process in CNS [60].

5. Conclusions

In this study, we first investigated toxic effects of TiO_2NPs on three individual cell lines. TiO_2NPs were mainly taken up by ALT and BV-2 cells, not by N2a. In addition, NPs were taken up via clathrin- and caveolae-dependent endocytosis in ALT and clathrin-dependent endocytosis and phagocytosis in BV-2, and needed 16 h to enter into lysosome, which may explain the slow production rate of intracellular ROS in the two cells. Moreover, TiO_2NPs induced H_2O_2 and cytokines release from BV-2, as well as LPS-activated BV-2. These results trigger our interests to further study the effects of TiO_2NPs with cell-cell interaction. By using Transwell system, we first demonstrated that it was difficult to detect TiO_2NPs in upper chamber N2a or BV-2 cells, which excluded direct NP effects. Then, we found that TiO_2NPs damaged N2a indirectly by high H_2O_2 and/or TNF-α release from LPS-activated BV-2 in the bottom chamber of Transwell. This indicates that the ability of TiO_2NPs to induce H_2O_2 or cytokines from microglia is a key factor for determining neurotoxicity, especially when the brain has already been injured. Neither N2a nor BV-2 were affected by indirect TiO_2NP or TiO_2NPs-LPS exposure to ALT-N2a or ALT-BV-2 co-culture, which suggests that indirect neuron damage would not be due mainly to TiO_2NP-astrocyte interaction.

Competing interests

The authors declare that they have no competing interests.

Acknowledgment

The authors acknowledge funding from the Ministry of Science and Technology (MOST), Taiwan (103-2221-E-007-006-MY3).

Transparency document

Transparency document related to this article can be found online at http://dx.doi.org/10.1016/j.cbi.2016.05.024

Appendix A. Supplementary data

Supplementary data related to this article can be found at http://dx.doi.org/10.1016/j.cbi.2016.05.024.

References

[1] S. Josset, N. Keller, M.C. Lett, M.J. Ledoux, V. Keller, Numeration methods for targeting photoactive materials in the UV-A photocatalytic removal of microorganisms, Chem. Soc. Rev. 37 (2008) 744–755.
[2] K. Kowal, P. Cronin, E. Dworniczek, J. Zeglinski, P. Tiernan, M. Wawrzynska, H. Podbielska, S.A.M. Tofail, Biocidal effect and durability of nano-TiO_2 coated textiles to combat hospital acquired infections, RSC Adv. 4 (2014) 19945–19952.
[3] N. Veronovski, M. Lesnik, A. Lubej, D. Verhovsek, Surface treated titanium dioxide nanoparticles as inorganic UV filters in sunscreen products, Acta. Chim. Slov. 61 (2014) 595–600.
[4] B. Bhushan, D. Luo, S.R. Schricker, W. Sigmund, S. Zauscher, Handbook of Nanomaterials Properties, Springer, 2014.
[5] X.X. Chen, B. Cheng, Y.X. Yang, A.N. Cao, J.H. Liu, L.J. Du, Y.F. Liu, Y.L. Zhao, H.F. Wang, Characterization and preliminary toxicity assay of nano-titanium dioxide additive in sugar-coated chewing gum, Small 9 (2013) 1765–1774.
[6] ICIS, Titanium Dioxide (TiO_2) Uses and Market Data, 2007.
[7] H.B. Shi, R. Magaye, V. Castranova, J.S. Zhao, Titanium dioxide nanoparticles: a review of current toxicological data, Part. Fibre. Toxicol. 10 (2013).
[8] Y.G. Ze, L. Sheng, X.Y. Zhao, J. Hong, X. Ze, X.H. Yu, X.Y. Pan, A. Lin, Y. Zhao, C. Zhang, Q.P. Zhou, L. Wang, F.S. Hong, TiO_2 nanoparticles induced hippocampal neuroinflammation in mice, PLoS One 9 (2014).
[9] R. Hu, X. Gong, Y. Duan, N. Li, Y. Che, Y. Cui, M. Zhou, C. Liu, H. Wang, F. Hong, Neurotoxicological effects and the impairment of spatial recognition memory in mice caused by exposure to TiO_2 nanoparticles, Biomaterials 31 (2010) 8043–8050.
[10] L. Geraets, A.G. Oomen, P. Krystek, N.R. Jacobsen, H. Wallin, M. Laurentie, H.W. Verharen, E.F.A. Brandon, W.H. de Jong, Tissue distribution and elimination after oral and intravenous administration of different titanium dioxide nanoparticles in rats, Part. Fibre. Toxicol. 11 (2014).
[11] C. Disdier, J. Devoy, A. Cosnefroy, M. Chalansonnet, N. Herlin-Boime, E. Brun, A. Lund, A. Mabondzo, Tissue biodistribution of intravenously administrated titanium dioxide nanoparticles revealed blood-brain barrier clearance and brain inflammation in rat, Part. Fibre. Toxicol. 12 (2015) 27.
[12] Y. Ze, R. Hu, X. Wang, X. Sang, X. Ze, B. Li, J. Su, Y. Wang, N. Guan, X. Zhao, S. Gui, L. Zhu, Z. Cheng, J. Cheng, L. Sheng, Q. Sun, L. Wang, F. Hong, Neurotoxicity and gene-expressed profile in brain-injured mice caused by exposure to titanium dioxide nanoparticles, J. Biomed. Mater. Res. A 102 (2014) 470–478.
[13] S.C. Liu, L.J. Xu, T. Zhang, G.G. Ren, Z. Yang, Oxidative stress and apoptosis induced by nanosized titanium dioxide in PC12 cells, Toxicology 267 (2010) 172–177.
[14] J. Wu, J.A. Sun, Y. Xue, Involvement of JNK and P53 activation in G2/M cell cycle arrest and apoptosis induced by titanium dioxide nanoparticles in neuron cells, Toxicol. Lett. 199 (2010) 269–276.
[15] L. Sheng, Y.G. Ze, L. Wang, X.H. Yu, J. Hong, X.Y. Zhao, X. Ze, D. Liu, B.Q. Xu, Y. Zhu, Y. Long, A.A. Lin, C. Zhang, Y. Zhao, F.H. Hong, Mechanisms of TiO_2 nanoparticle-induced neuronal apoptosis in rat primary cultured hippocampal neurons, J. Biomed. Mater. Res. A 103 (2015) 1141–1149.
[16] T.C. Long, N. Saleh, R.D. Tilton, G.V. Lowry, B. Veronesi, Titanium dioxide (P25) produces reactive oxygen species in immortalized brain microglia (BV2): implications for nanoparticle neurotoxicity, Environ. Sci. Technol. 40 (2006) 4346–4352.
[17] Y.F. Liu, Z. Xu, X.D. Li, Cytotoxicity of titanium dioxide nanoparticles in rat neuroglia cells, Brain Inj. 27 (2013) 934–939.
[18] V. Valdiglesias, C. Costa, V. Sharma, G. Kilic, E. Pasaro, J.P. Teixeira, A. Dhawan, B. Laffon, Comparative study on effects of two different types of titanium dioxide nanoparticles on human neuronal cells, Food Chem. Toxicol. 57 (2013) 352–361.
[19] S.G. Marquez-Ramirez, N.L. Delgado-Buenrostro, Y.I. Chirino, G.G. Iglesias, R. Lopez-Marure, Titanium dioxide nanoparticles inhibit proliferation and induce morphological changes and apoptosis in glial cells, Toxicology 302 (2012) 146–156.
[20] E. Huerta-Garcia, J.A. Perez-Arizti, S.G. Marquez-Ramirez, N.L. Delgado-Buenrostro, Y.I. Chirino, G.G. Iglesias, R. Lopez-Marure, Titanium dioxide nanoparticles induce strong oxidative stress and mitochondrial damage in glial cells, Free Radic. Biol. Med. 73 (2014) 84–94.
[21] A.Y. Abramov, L. Canevari, M.R. Duchen, Calcium signals induced by amyloid beta peptide and their consequences in neurons and astrocytes in culture, Biochim. Biophys. Acta 1742 (2004) 81–87.
[22] P.R. Angelova, A.Y. Abramov, Interaction of neurons and astrocytes underlies the mechanism of Abeta-induced neurotoxicity, Biochem. Soc. Trans. 42 (2014) 1286–1290.
[23] C.K. Combs, J.C. Karlo, S.C. Kao, G.E. Landreth, Beta-Amyloid stimulation of microglia and monocytes results in TNFalpha-dependent expression of inducible nitric oxide synthase and neuronal apoptosis, J. Neurosci. 21 (2001) 1179–1188.

[24] E.S. Jung, K. An, H.S. Hong, J.H. Kim, I. Mook-Jung, Astrocyte-originated ATP protects Abeta(1-42)-induced impairment of synaptic plasticity, J. Neurosci. 32 (2012) 3081–3087.
[25] D. Davalos, J. Grutzendler, G. Yang, J.V. Kim, Y. Zuo, S. Jung, D.R. Littman, M.L. Dustin, W.B. Gan, ATP mediates rapid microglial response to local brain injury in vivo, Nat. Neurosci. 8 (2005) 752–758.
[26] M.R. Pickard, D.M. Chari, Robust uptake of magnetic nanoparticles (MNPs) by central nervous system (CNS) microglia: implications for particle uptake in mixed neural cell populations, Int. J. Mol. Sci. 11 (2010) 967–981.
[27] A. Haase, S. Rott, A. Mantion, P. Graf, J. Plendl, A.F. Thunemann, W.P. Meier, A. Taubert, A. Luch, G. Reiser, Effects of silver nanoparticles on primary mixed neural cell cultures: uptake, oxidative stress and acute calcium responses, Toxicol. Sci. 126 (2012) 457–468.
[28] Y. Xue, J. Wu, J. Sun, Four types of inorganic nanoparticles stimulate the inflammatory reaction in brain microglia and damage neurons in vitro, Toxicol. Lett. 214 (2012) 91–98.
[29] T.C. Long, J. Tajuba, P. Sama, N. Saleh, C. Swartz, J. Parker, S. Hester, G.V. Lowry, B. Veronesi, Nanosize titanium dioxide stimulates reactive oxygen species in brain microglia and damages neurons in vitro, Environ. Health Perspect. 115 (2007) 1631–1637.
[30] S.T. Stern, P.P. Adiseshaiah, R.M. Crist, Autophagy and lysosomal dysfunction as emerging mechanisms of nanomaterial toxicity, Part. Fibre Toxicol. 9 (2012) 16.
[31] C.Y. Wu, K.J. Tu, C.H. Wu, High hydroxyl group density on the surface of TiO_2 pretreated with alkaline hydrogen peroxide, Abstr. Pap. Am. Chem. S 246 (2013).
[32] Y.M. Leung, C.F. Huang, C.C. Chao, D.Y. Lu, C.S. Kuo, T.H. Cheng, L.Y. Chang, C.H. Chou, Voltage-gated K+ channels play a role in cAMP-stimulated neuritogenesis in mouse neuroblastoma N2A cells, J. Cell. Physiol. 226 (2011) 1090–1098.
[33] S. Herculano-Houzel, The glia/neuron ratio: how it varies uniformly across brain structures and species and what that means for brain physiology and evolution, Glia 62 (2014) 1377–1391.
[34] W. Liu, Y. Tang, J. Feng, Cross talk between activation of microglia and astrocytes in pathological conditions in the central nervous system, Life Sci. 89 (2011) 141–146.
[35] H. Suzuki, T. Toyooka, Y. Ibuki, Simple and easy method to evaluate uptake potential of nanoparticles in mammalian cells using a flow cytometric light scatter analysis, Environ. Sci. Technol. 41 (2007) 3018–3024.
[36] Y. Toduka, T. Toyooka, Y. Ibuki, Flow cytometric evaluation of nanoparticles using side-scattered light and reactive oxygen species-mediated fluorescence-correlation with genotoxicity, Environ. Sci. Technol. 46 (2012) 7629–7636.
[37] E. Radi, P. Formichi, C. Battisti, A. Federico, Apoptosis and oxidative stress in neurodegenerative diseases, J. Alzheimers Dis. 42 (Suppl. 3) (2014) S125–S152.
[38] J. Rejman, V. Oberle, I.S. Zuhorn, D. Hoekstra, Size-dependent internalization of particles via the pathways of clathrin-and caveolae-mediated endocytosis, Biochem. J. 377 (2004) 159–169.
[39] M.K. Zenni, P.C. Giardina, H.A. Harvey, J.Q. Shao, M.R. Ketterer, D.M. Lubaroff, R.D. Williams, M.A. Apicella, Macropinocytosis as a mechanism of entry into primary human urethral epithelial cells by Neisseria gonorrhoeae, Infect. Immun. 68 (2000) 1696–1699.
[40] H. Nohl, L. Gille, Lysosomal ROS formation, Redox Rep. Commun. Free Radic. Res. 10 (2005) 199–205.
[41] R.M. Zucker, E.J. Massaro, K.M. Sanders, L.L. Degn, W.K. Boyes, Detection of TiO_2 nanoparticles in cells by flow cytometry, Cytom. Part A 77A (2010) 677–685.
[42] V. Zujovic, V. Taupin, Use of cocultured cell systems to elucidate chemokine-dependent neuronal/microglial interactions: control of microglial activation, Methods 29 (2003) 345–350.
[43] F. Cengelli, D. Maysinger, F. Tschudi-Monnet, X. Montet, C. Corot, A. Petri-Fink, H. Hofmann, L. Juillerat-Jeanneret, Interaction of functionalized superparamagnetic iron oxide nanoparticles with brain structures, J. Pharmacol. Exp. Ther. 318 (2006) 108–116.
[44] H.Y. Wu, M.C. Chung, C.C. Wang, C.H. Huang, H.J. Liang, T.R. Jan, Iron oxide nanoparticles suppress the production of IL-1beta via the secretory lysosomal pathway in murine microglial cells, Part. Fibre Toxicol. 10 (2013).
[45] M.G. Bianchi, M. Allegri, A.L. Costa, M. Blosi, D. Gardini, C. Del Pivo, A. Prina-Mello, L. Di Cristo, O. Bussolati, E. Bergamaschi, Titanium dioxide nanoparticles enhance macrophage activation by LPS through a TLR4-dependent intracellular pathway, Toxicol. Res. UK 4 (2015) 385–398.
[46] F.T. Crews, R.P. Vetreno, Addiction, adolescence, and innate immune gene induction, Front Psychiatry 2 (2011) 19.
[47] M.E. Heid, P.A. Keyel, C. Kamga, S. Shiva, S.C. Watkins, R.D. Salter, Mitochondrial reactive oxygen species induces NLRP3-dependent lysosomal damage and inflammasome activation, J. Immunol. 191 (2013) 5230–5238.
[48] J.L. Mason, K. Suzuki, D.D. Chaplin, G.K. Matsushima, Interleukin-1 beta promotes repair of the CNS, J. Neurosci. 21 (2001) 7046–7052.
[49] Y. Zorina, R. Iyengar, K.D. Bromberg, Cannabinoid 1 receptor and interleukin-6 receptor together induce integration of protein kinase and transcription factor signaling to trigger neurite outgrowth, J. Biol. Chem. 285 (2010) 1358–1370.
[50] C. Ali, O. Nicole, F. Docagne, S. Lesne, E.T. MacKenzie, A. Nouvelot, A. Buisson, D. Vivien, Ischemia-induced interleukin-6 as a potential endogenous neuroprotective cytokine against NMDA receptor-mediated excitotoxicity in the brain, J. Cereb. Blood Flow. Metab. 20 (2000) 956–966.
[51] S.A. Loddick, A.V. Turnbull, N.J. Rothwell, Cerebral interleukin-6 is neuroprotective during permanent focal cerebral ischemia in the rat, J. Cereb. Blood Flow. Metab. 18 (1998) 176–179.
[52] J.A. Smith, A. Das, S.K. Ray, N.L. Banik, Role of pro-inflammatory cytokines released from microglia in neurodegenerative diseases, Brain Res. Bull. 87 (2012) 10–20.
[53] A.L.D. Ezcurra, M. Chertoff, C. Ferrari, M. Graciarena, F. Pitossi, Chronic expression of low levels of tumor necrosis factor-alpha in the substantia nigra elicits progressive neurodegeneration, delayed motor symptoms and microglia/macrophage activation, Neurobiol. Dis. 37 (2010) 630–640.
[54] R. Fu, Q. Shen, P. Xu, J.J. Luo, Y. Tang, Phagocytosis of microglia in the central nervous system diseases, Mol. Neurobiol. 49 (2014) 1422–1434.
[55] M.J. Geisow, P.D. Hart, M.R. Young, Temporal changes of lysosome and phagosome Ph during phagolysosome formation in macrophages - studies by fluorescence spectroscopy, J. Cell. Biol. 89 (1981) 645–652.
[56] C.F. Orr, D.B. Rowe, G.M. Halliday, An inflammatory review of Parkinson's disease, Prog. Neurobiol. 68 (2002) 325–340.
[57] L. Chen, L. Liu, J. Yin, Y. Luo, S. Huang, Hydrogen peroxide-induced neuronal apoptosis is associated with inhibition of protein phosphatase 2A and 5, leading to activation of MAPK pathway, Int. J. Biochem. Cell B 41 (2009) 1284–1295.
[58] A.K. Talley, S. Dewhurst, S.W. Perry, S.C. Dollard, S. Gummuluru, S.M. Fine, D. New, L.G. Epstein, H.E. Gendelman, H.A. Gelbard, Tumor necrosis factor alpha-induced apoptosis in human neuronal cells: protection by the antioxidant N-acetylcysteine and the genes bcl-2 and crmA, Mol. Cell. Biol. 15 (1995) 2359–2366.
[59] C. Verderio, M. Matteoli, ATP mediates calcium signaling between astrocytes and microglial cells: modulation by IFN-gamma, J. Immunol. 166 (2001) 6383–6391.
[60] I. Hide, M. Tanaka, A. Inoue, K. Nakajima, S. Kohsaka, K. Inoue, Y. Nakata, Extracellular ATP triggers tumor necrosis factor-alpha release from rat microglia, J. Neurochem. 75 (2000) 965–972.